Open Access

*Journal of Energy and Power Technology*

LIDSEN Publishing Inc.

Original Research

# An Adsorption-Desorption Heat Engine for Power Generation from Waste Heat

Mikhail Granovskiy *

Professional Engineers of Ontario, Canada; E-Mail: mgranovskii@gmail.com

* **Correspondence:** Mikhail Granovskiy; E-Mail: mgranovskii@gmail.com

**Academic Editor:** Kiari Goni Boulama

**Special Issue**: Applied Thermodynamics and Energy Conversion

*Journal of Energy and Power Technology*
2023, volume 5, issue 4
doi:10.21926/jept.2304034

**Received:** October 17, 2023
**Accepted:** November 09, 2023
**Published:** November 14, 2023

**Abstract**

According to the United States Department of Energy, waste heat recovery would allow up to a 20% reduction in greenhouse gases (GHG) emission. Most of the waste energy is discharged as a low-grade heat at temperatures less than 250°C. Therefore, the development of new technologies and the enhancement of existing ones to convert low-grade heat into electrical or mechanical energy are of great importance. The working principle of adsorption-desorption heat pumps with cyclic switching between adsorption and desorption is adapted in the proposed heat engine to generate electrical power from low-temperature heat. Thermodynamic analysis of the heat engine cycle is carried out for the pair adsorbant-adsorbent: $CO_2$-activated carbon. Its efficiencies are calculated accepting the ideal gas law and an adsorption-desorption equilibrium at the key points of the cycle. The cycle consists of two isochores and two isotherms like the Stirling engine, but at the same temperature range and without heat regeneration, its thermal efficiency (work per heat supplied) can reach 11.3% vs. 5.0% and specific work $50.7\frac{kJ}{kg\_CO2}$ vs. $3.55\frac{kJ}{kg\_CO2}$ in the latter. The proposed unit has thermal efficiency in the range of Organic Rankine Cycle units and can be utilized in small-scale applications up to 40kWe, where manufacturing cost of turbines or expanders for ORCs increases dramatically. Accounting for quality (temperature)

of utilized heat, the proposed cycle's exergy efficiency, $\zeta_{ex}$ = 34.5% approaches that of water-steam Rankine cycles utilizing natural gas or coal combustion.

**Keywords**
Heat engine; thermodynamic cycle; waste heat; exergy analysis; adsorption-desorption; Stirling engine

## 1. Introduction

Organic Rankine Cycle (ORC) heat engines, which use organic liquids instead of water as their working fluids, are the most cited in processes of low-potential waste heat (≤250°C) utilization [1]. These engines employ indirect heat transfer to evaporate (at higher pressure) and condense (at lower pressure) organic liquids. The highest pressure in the cycle is produced by a pump forcing liquid to flow from condenser to evaporator. The vapor obtained in the evaporator expands to the lowest pressure in a turbine that generates mechanical work for the subsequent conversion into power via electric generator.

The working fluid of the cycle accepts and releases heat indirectly, "through the wall" in the evaporator and condenser, respectively. The latent heat transfer is relatively fast, as evaporation and condensation are characterized with the highest heat transfer coefficients. Organic liquids, due to their low boiling points compared to water, evaporate at lower temperatures to accept low-potential, usually sensible heat from external gases and liquids.

ORC cycles are not robust for small-scale applications up to 40 kWe, because the rotating speed of their turbines significantly increases with decreasing turbine output power [1, 2], while their manufacturing costs per kW of produced energy increases dramatically [2, 3].

Conventional Stirling engines also employ indirect heat transfer to gaseous working fluids but permit low-kilowatt power generation. Pistons force gas to move between hot and cold zones within one or two connected cylinders. The kinematic mechanism generates extra mechanical work because gas makes greater mechanical work in its heating and expansion than it consumes in its cooling and contraction. The intensity and efficiency of heat transfer is inferior to that of ORC heat engines. Therefore, Stirling engines require a substantial temperature gradient between heat source and sink [4]. As the literature [5] indicates, they can operate efficiently only if the thermal energy source is at temperatures indicatively higher than 300°C, challenging high temperature sealing requirements. Presently, Stirling engines are associated with low on-site operational efficiencies and high manufacturing costs [6].

Recently, the adsorption phenomenon has received increasing attention for employment in sorption heat pumps utilizing low-temperature waste heat. This waste heat is used to desorb refrigerant vapor from adsorbent to allow its adsorption at the next stage, yielding a cooling effect caused by refrigerant evaporation [7, 8]. Sorption heat pumps do not require compressors and electricity to run; there is no vibration of moving parts with an associated tendency of their breakage. Allowing a continuous operation, semi-batch units consist of two identical reactors (adsorber and desorber) and heat exchangers (evaporator and condenser), switching their functionalities during the process.

The possibility of reversible chemical and physical processes to produce electricity from low temperature heat was studied in a few publications and rather overlooked. Nomura et al. [9] proposed a chemical engine that used the reversible reaction of hydrogen with metals to form metal hydrides. Hydrogen released from metal hydride (with an uptake of heat) at high pressure and temperature was used to turn the work generating mechanism. At the exit, hydrogen was absorbed by the metal (with a discharge of heat) to allow repeating the process again. The proposed semi-batch unit (with a constant heat supply and withdrawal) required strict synchronization of direct and reverse reaction kinetics with the rotation speed of the work generating mechanism.

Bao et al. [10] numerically investigated for the first time the novel combination of the chemisorption cycle and the scroll expander for refrigeration and power cogeneration. However, because of the mutual constraint between the chemisorption and the expansion when they link in series, the power output of the cogeneration mode was only around one third of the original expectation.

Muller and Schulze-Makuch [11] presented the idea of a sorption heat engine. They described a batch adsorber where adsorbant gas was firstly desorbed (with a heat uptake), expanded to generate work, and readsorbed back (with a heat discharge) to repeat the process again. Periodic heat supply and withdrawal should be synchronized with the corresponding stage. The described process was not thermodynamically analyzed to obtain its performance indicators and, subsequently, define its efficiency.

Here, the author extends the above-mentioned idea to an adsorption-desorption semi-batch unit to generate power from a low-grade waste heat. A distinctive feature of the unit is the absence of mass transfer (gas flow) between desorber and adsorber. A detailed thermodynamic analysis is carried out to compare its performance with Stirling, Carnot, ORC, and Rankine cycles.

## 2. An Adsorption-Desorption Heat Engine

### *2.1 A Configuration of an Adsorption-Desorption Heat Engine*

A principal schematic of an adsorption-desorption heat engine is presented in Figure 1. Adsorber and desorber are identical devices accommodating two coiled heat exchangers. Adsorbent tubes and one heat exchanger are submerged into a low-boiling point heat transfer liquid (for instance, n-pentane, which is frequently used in ORC cycles [12]).

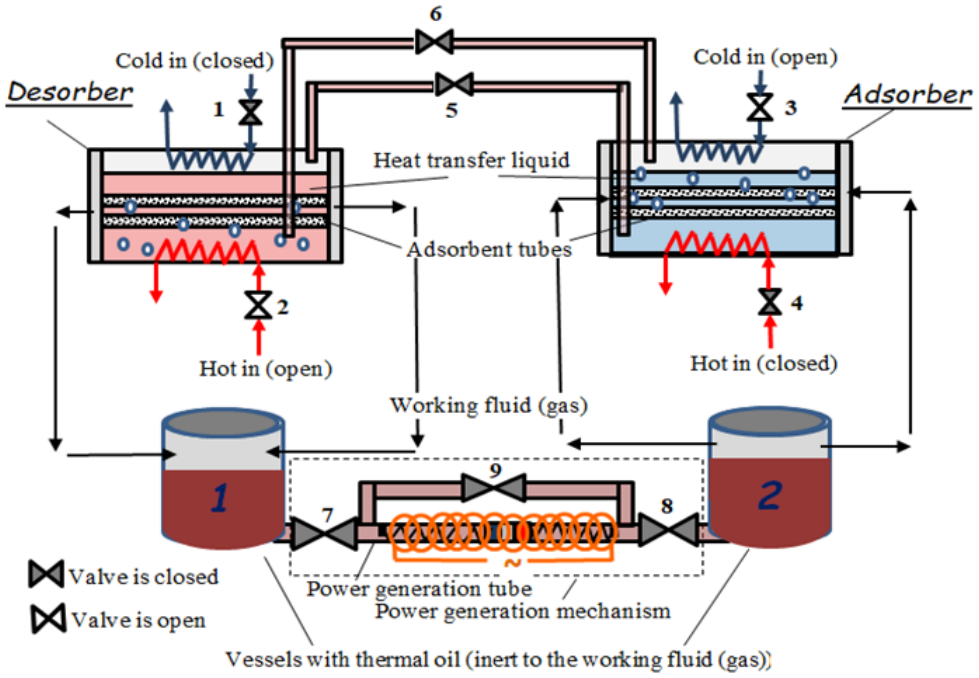


**Figure 1** A principle schematic of an adsorption-desorption heat engine.

Adsorber and desorber are physically linked through two vessels with an inert high-boiling point thermal oil (for instance, Duratherm LT [13], with a boiling point higher than 589 K) and a power generation mechanism incorporating one or more power generation tubes. A power generation tube consists of a permanent piston-magnet sliding along a cylindrical tube, stretching one spring and compressing another in response to a pressure difference in two vessels at open Valves 7 and 8 and closed Valve 9.

### *2.2 The Principles of Electricity Production and Heat Regeneration*

In desorber, a hot gas (waste heat carrier) enters the bottom heat exchanger (Valve 2 is open, Valve 1 is closed) and vaporizes n-pentane. This vapor condenses on outer surfaces of adsorbent tubes with a heat release causing adsorbant gas to desorb. With Valves 5, 6, and 7 closed (Figure 1), the pressure of the gas in Vessel_1 increases.

In adsorber, n-pentane is vaporized near adsorbent tubes where exothermic (heat releasing) adsorption takes place. A cooling water or air enters the top heat exchanger (cooler) (Valve 3 is open, Valve 4 is closed) to condense vapor and maintain a temperature to advance adsorption. With Valves 5, 6, and 8 closed Figure 1), the pressure of the gas in Vessel_2 decreases.

When desorption and adsorption approach their equilibriums in desorber and adsorber, Valves 7 and 8 get opened, while Valve 9 is closed. Due to higher gas pressure in Vessel_1, thermal oil pushes a piston-magnet to the right, stretching and compressing the left and right springs, respectively (Figure 2).

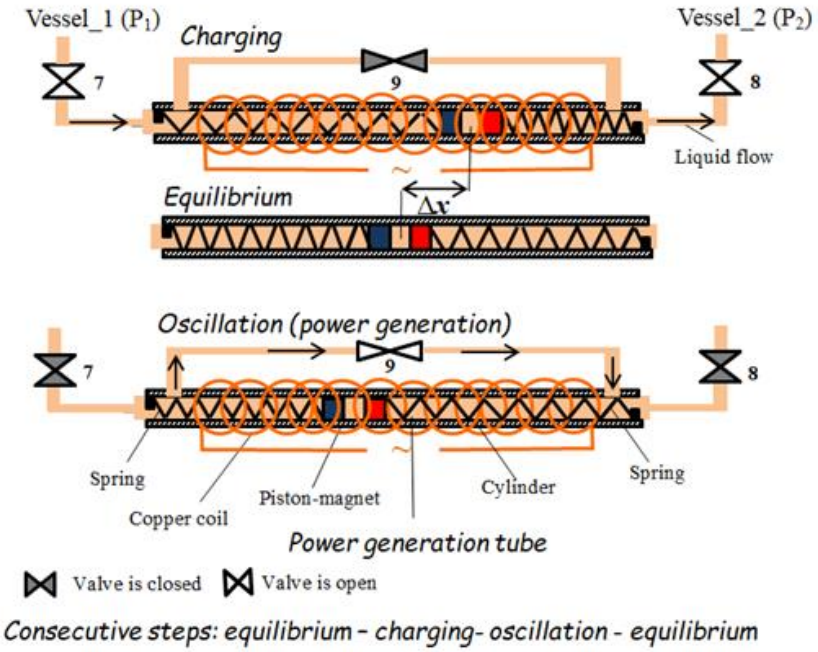


**Figure 2** A principle of power generation in the adsorption-desorption heat engine.

Due to an increase in gas volume, the pressure in desorber and Vessel_1 decreases. This promotes further gas desorption. A continuous heat uptake by adsorbent is provided by a corresponding heat supply that maintains near-isothermal conditions.

Due to a respective decrease in gas volume, the pressure in adsorber and Vessel_2 increases. This promotes further gas adsorption and heat release. A continuous heat removal from adsorbent is provided by corresponding condensation of saturated n-pentane vapor via cooling air or water that also maintains near-isothermal conditions. The temperature in adsorber is lower than in desorber.

At a designed pressure difference in vessels, Valves 7 and 8 get closed and Valve 9 gets opened (Figure 2). Continuous conversion between potential and kinetic energy of springs induces back and forth movements (oscillations) of a piston-magnet. These oscillations generate a variable magnetic field and alternate electric current in a wire spiraled around the tube.

This current can be directed to and collected by an energy storage device (battery or capacitor). For instance, in Figure 3, a well-known diode bridge converts alternate current into a direct one, and the latter charges a capacitor or battery coupled with the load. Amplitudes of piston-magnet oscillations as well as current (voltage) attenuate during this process. When piston-magnet oscillations are practically over, Valve 9 gets closed.

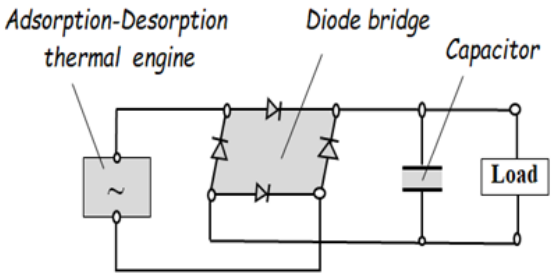


**Figure 3** A principal scheme of an energy storage device (capacitor) charging.

Valves 7 and 8 get closed after charging the power generation mechanism; then, the latter becomes separated from adsorber and desorber, and switching desorber and adsorber functionalities occur (Valves 1 and 4 are open; Valves 2 and 3 are closed; see Figure 1). This switching starts with the heat regeneration. If desorber is on the left (as in Figure 1), Valve 5 gets opened; if it is on the right, Valve 6 gets opened. A high pressure and high temperature vapor flows from desorber to adsorber. It condenses within a relatively cold liquid in adsorber and heats it and adsorbent up, causing an inception of gas desorption there and preparing adsorber to be desorber at this stage. A decrease in vapor pressure in desorber induces spontaneous liquid vaporization and declination in liquid and adsorbent temperatures, causing an inception of gas adsorption there and preparing desorber to be adsorber at this stage. When both devices reach the same vapor pressure, Valve 5 (or 6) gets closed, and the system starts a new power generation cycle.

## 3. Thermodynamic Analysis of Adsorption-Desorption Heat Engine: A Case Study

### *3.1 A Source of Waste Heat: Air at 500 K (227°C)*

The temperature of 500 K is within a usual temperature range for flue gases from a typical boiler. The adsorption-desorption heat engine (as any heat engine) generates work from the heat that is supplied at higher temperatures and withdrawn at lower temperatures. If n-pentane vapor pressure in adsorber is kept 1 Bar, it boils and absorbs heat at 309 K [14]. The produced vapor is condensed in the top heat exchanger (cooler) to control the vapor pressure and release heat to ambient air or cooling water. An ambience (ambient air) is considered a universal heat sink, and its temperature is often taken equal to $T_0$ = 298 K [15].

The waste heat is transferred to adsorbent in desorber. This transfer includes boiling liquid n-pentane and condensing its vapor on adsorbent tubes. The following analysis allows finding an optimal boiling temperature for n-pentane in desorber.

When hot air cools down from $T_{in}$ = 500 K to an output temperature $T_{out}$ it transfer heat $Q_{Air}$ as follows:

$$Q_{air} = C_p^{air}(T_{in} - T_{out}) \quad (1)$$

where $C_p^{air}$ is the isobaric heat capacity of air (29.2 J/mol·K).

The exergy of $Q_{air}$ is defined as the maximum work that can be obtained in the ideal Carnot engine with a heat sink temperature $T_0$. This exergy $E_{air}$ is determined as follows:

$$E_{air} = Q_{air}\left(1 - {}^{T_0}/_{T^*}\right) \tag{2}$$

where $T^*$ is an average thermodynamic temperature reflecting air cooling from $T_{in}$ to $T_{out}$ as follows:

$$T^* = \frac{\int_{T_{in}}^{T_{out}} dH_{air}}{\int_{T_{in}}^{T_{out}} dS_{air}} = \frac{\int_{T_{out}}^{T_{in}} C_p^{air} dT}{\int_{T_{out}}^{T_{in}} \frac{C_p^{air}}{T} dT} = \frac{T_{in} - T_{out}}{\ln \frac{T_{in}}{T_{out}}} \tag{3}$$

where $dH_{air}$ and $dS_{air}$ are differential changes in air enthalpy and entropy along with the transfer of sensible heat. Figure 4 shows that with decreasing $T_{out}$ the difference between energy (heat) and exergy (ability to generate work) increases.

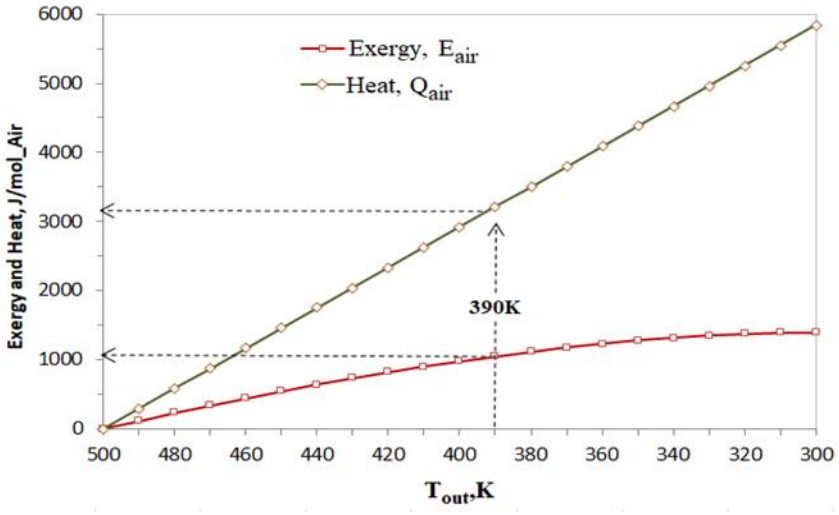


**Figure 4** The exergy and heat transferred from air ($T_{in}$ = 500 K) as a function of output temperature $T_{out}$.

If n-pentane boils at temperature $T_{out}$ it absorbs sensible heat of air $Q_{air}$ (see Eq. (1)) in the range of $T_{in}$ = 500 K to $T_{out}$ to produce saturated vapor at $T_{out}$. The exergy of saturated vapor that condenses and releases heat at $T_{out}$ on adsorbent tubes is expressed as follows:

$$E_{sv} = Q_{air}\left(1 - \frac{T_0}{T_{out}}\right) \tag{4}$$

Exergy of saturated vapour $E_{sv}$ in equation (4) is a product of two terms. The first term $Q_{air}$ increases with decreasing $T_{out}$ as shown in Figure 4 and expressed by equation (1). The second term $\left(1 - \frac{T_0}{T_{out}}\right)$ decreases with decreasing $T_{out}$ (to $T_0$). The behavior of two terms points out a product function with an extreme. Exergy of saturated vapour $E_{sv}$ as a function of $T_{out}$ (Figure 5) has a maximum of $T_{out}$ = 390 K. This exergy is transferred to adsorbent. To maintain this temperature, the corresponding n-pentane pressure in desorber should be 8.5 Bar [13]. The average thermodynamic temperature of air that cools down from 500 K to 390 K is $T^*$ = 443 K [Eq. (3)].

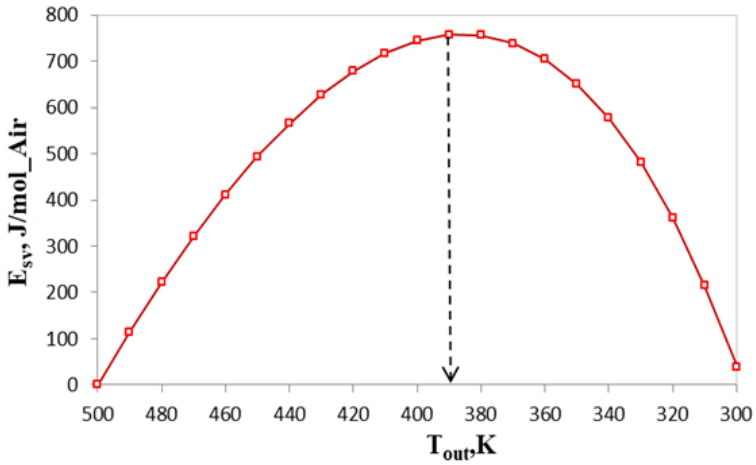


**Figure 5** Exergy of saturated vapour $E_{sv}$ as a function of outlet air temperature $T_{out}$.

### *3.2 Adsorbent-Adsorbate Pair: Activated Carbon and $CO_2$*

3.2.1 An Isotherm of $CO_2$ Adsorption on Activated Carbon (AC)

A widely used activated carbon (AC) (Maxsorb-III) and $CO_2$ gas are chosen as an adsorbent-adsorbate pair. The fitting parameters for the Tóth isotherm equation are taken from [16] (see Table 1):

$$q = \frac{q_0 bP}{((1 + (bP)^t)^{1/t}} \tag{5}$$

where q denotes the absolute mass of $CO_2$ adsorbed by unit mass of adsorbent (kg/kg adsorbent at equilibrium state); $q_0$ is the saturated amount adsorbed (kg/kg); t is the heterogeneity parameter; and b is the adsorption affinity ($kPa^{-1}$), given by:

$$b = b_0 \exp\left(\frac{Q}{RT}\right) \tag{6}$$

where $b_0$ is the adsorption affinity at infinite temperature ($kPa^{-1}$), and Q is the isosteric heat of adsorption (J/mol).

**Table 1** Parameters for Tóth isotherm equation.

| **$q_0$**, kg/kg | **$b_0$**, $kPa^{-1}$ | **Q**, J/mol | **t** |
|---|---|---|---|
| 2.3601 | $1.842 \times 10^{-7}$ | 19297 | 0.799 |

Based on the Tóth equation, three isobars of adsorption are presented in Figure 6.

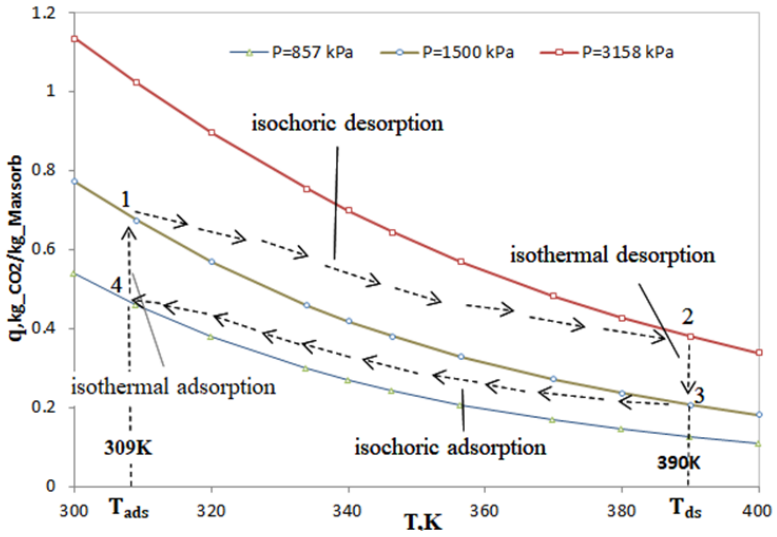


**Figure 6** An adsorption-desorption thermodynamic cycle (1-2-3-4). The points and arrows denote the thermodynamic trajectory of the cycle.

3.2.2 Adsorption-Desorption Thermodynamic Cycle

The pressure $P_{eq}$ = 1500 kPa at which gas expansion in desorber equilibrates with its compression in adsorber at open Valves 7 and 8 (Figure 1 and Figure 2) is taken as a starting point for the cycle simulation. Note that the validity of formulas (5) and (6) includes this value.

The adsorption-desorption thermodynamic cycle is presented in Figure 6 and Figure 7 (1-2-3-4) in q-T and P-V coordinates, respectively. As seen in Figure 6 and Figure 7, Points 1 and 3 correspond to adsorption equilibriums at the same pressure $P_{eq}$ = 1500 kPa but different temperatures: $T_{ads}$ = 309 K at Point 1 in adsorber and $T_{ds}$ = 390 K at Point 3 in desorber. At these points, isothermal expansion and desorption and isothermal compression and adsorption attain equal pressures. To continue, desorption and adsorption must switch. Technically, this means that Valves 7 and 8 get closed, and desorber and adsorber exchange their functionalities by starting up heat regeneration and redirection of heating and cooling flows (see Chapters 2.1 and 2.2).

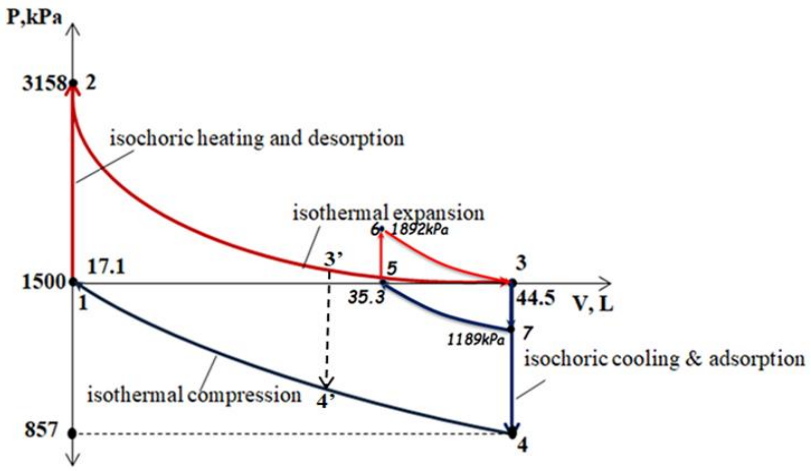


**Figure 7** Thermodynamic trajectory of adsorption-desorption (1-2-3-4) and Stirling (6-3-7-5) cycles in **P-V** coordinates. Thermodynamic trajectory of adsorption-desorption cycle (1-2-3'-4') is for a specific mechanical load (see the text).

Then, adsorbent in desorber is isochorically heated from $T_{ads}$ = 309 K at Point 1 to $T_{ds}$ = 390 K at Point 2, reaching adsorption equilibrium at the elevated pressure. Adsorbent in adsorber is cooled from $T_{ds}$ = 390 K at Point 3 to $T_{ads}$ = 309 K at Point 4, reaching adsorption equilibrium at the lower pressure. After reaching isochoric equilibriums, Valves 7, 8 open to proceed with isothermal expansion 2-3 and isothermal compression 4-1 in desorber and adsorber, respectively.

The difference in the gas amounts (desorbed $CO_2$) corresponding to full desorption and adsorption at Points 3 and 1 is ΔN = 10.6 mol/kg_AC (see Figure 6, where q is the mass of adsorbed $CO_2$). Another parameter, $N_{min}$, is needed for the cycle simulation. It is a molar quantity of $CO_2$ that permanently remains in gas. For instance, if $N_{min}$ = 10 mol/kg_AC, the gas phase is comprised of 10 mol of $CO_2$ after complete adsorption (Point 1) and 20.6 mol of $CO_2$ after complete desorption (Point 3) per 1 kg of adsorbent, as in adsorber and desorber.

The minimum gas volume in adsorber after isothermal compression at Point 1 is defined by the Clapeyron-Mendeleev equation as follows:

$$\mathrm{N_1 = N_{min}; P_1 = P_{eq}} \tag{7}$$

$$\mathrm{V_1 = V_{min} = \frac{N_{min} R T_{ads}}{P_{eq}} = 17.1 L} \tag{8}$$

Similarly, the maximum gas volume in desorber (after isothermal expansion) at Point 3 is as follows:

$$N_3 = N_{max} = N_{min} + \Delta N; \mathrm{P_3 = P_{eq}} \tag{9}$$

$$\mathrm{V_3 = V_{max} = \frac{N_{max} R T_{ds}}{P_{eq}} = 44.5\ L} \tag{10}$$

Thermodynamic parameters at Point 2 (pressure $P_2$ and $CO_2$ quantity $N_2$) are obtained using isochoric desorption at constant volume $V_{min}$ with increasing temperature from $T_1$ ($T_1 = T_{ads}$) to $T_2$ ($T_2 = T_{ds}$) and pressure from $P_{eq}$ to $P_2$. The Clapeyron-Mendeleev equation connects $P_2$ and $N_2$ as follows:

$$\mathrm{V_2 = V_{min}; P_2 = \frac{N_2 R T_{ds}}{V_{min}}} \tag{11}$$

The thermodynamic desorption equilibrium is described by Formulas (5) and (6). This is another correlation between two unknowns, $P_2$ and $N_2$ (through q), to determine their values.

Similarly, thermodynamic parameters at Point 4 (pressure, $P_4$ and $CO_2$ quantity, $N_4$) are obtained using isochoric adsorption at constant volume $V_{max}$ with decreasing temperature from $T_3$ ($T_3 = T_{ds}$) to $T_4$ ($T_4 = T_{ads}$) and pressure from $P_{eq}$ to $P_4$. The Clapeyron-Mendeleev equation connects $P_4$ and $N_4$ as follows:

$$\mathrm{V_4 = V_{max}}; P_4 = \frac{N_4 R T_{ads}}{V_{max}} \tag{12}$$

The thermodynamic adsorption equilibrium is also described by Formulas (5) and (6). This is another correlation between two unknowns, $P_4$ and $N_4$ (through q), to determine their values.

The calculated parameters of the thermodynamic cycle in Figure 6 and Figure 7 are listed in Table 2.

**Table 2** Parameters of adsorption-desorption thermodynamic cycle in Figure 6 and Figure 7.

| Point \ Parameters | **N** in gas, **mol/kg_AC** | **n** in AC, **mol/kg_AC** | **P**, **kPa** | **V, L** | **T, K** |
|---|---|---|---|---|---|
| Point 1* | 10.0 | 15.3 | 1500 | 17.1 | 309 |
| Point 2 | 16.7 | 8.6 | 3158 | 17.1 | 390 |
| Point 3** | 20.6 | 4.7 | 1500 | 44.5 | 390 |
| Point 4 | 14.9 | 10.4 | 857 | 44.5 | 309 |

*switching adsorber to desorber; **switching desorber to adsorber

3.2.3 Energy Balance of Adsorption-Desorption Cycle and Its Efficiency

The heat released during adsorption is equal to that consumed during desorption, as follows:

$$\Delta H_{ds} = -\Delta H_{ads} = Q \tag{13}$$

For desorption, a molar enthalpy difference is associated with heat consumption as follows:

$$\Delta H_{ds} = H_{CO2} - H_{CO2-AC} = C_v(T - T_0) + P\Delta V - H_{CO2-AC} \tag{14}$$

where $H_{CO2}$ is molar enthalpy of $CO_2$ in the gas; $H_{CO2\text{-}AC}$ is molar enthalpy of $CO_2$ in adsorbent; $C_v$ is $CO_2$ isochoric heat capacity ($C_v$ = 29.0 J/mol·K); $T_o$ = 298 K is a standard reference temperature; P is pressure; and ΔV is the volume change caused by desorption of one mol of $CO_2$.

Considering the adsorbed $CO_2$ as an incompressible substance referring to liquids or solids, its enthalpy $H_{CO2\text{-}AC}$ is equal to its internal energy $I_{CO2\text{-}AC}$. Accounting for $P\Delta V = RT$, molar $H_{CO2\text{-}AC}$ and $I_{CO2\text{-}AC}$ can be obtained from (14) as follows:

$$H_{CO2-AC} = I_{CO2-AC}(T) = C_v(T - T_0) + RT - \Delta H_{ds} \tag{15}$$

It is commonly accepted that isosteric heat of adsorption or desorption (calculated using the Clausius-Clapeyron equation) is independent of temperature [17]; in our case, it equals 19,297 J/mol (see Table 1). Based on Formula (15), the internal energies have the following values:

$$I_{CO2-AC}(T = T_{ds} = 390^oK) = -13387\ J/mol; I_{CO2-AC}(T = T_{ads} = 309^oK) = -16409\ J/mol \tag{16}$$

The heat consumed at isochoric heating along with desorption (Points 1-2) induces an increase in internal energy as follows:

$$\begin{aligned} Q_{1-2} &= \Delta I_{1-2} \\ &= [n_2 I_{CO2-AC}(T_2) + N_2 C_v(T_2 - T_0) + m_{AC} C_{AC}(T_2 - T_0)] \\ &\quad -[n_1 I_{CO2-AC}(T_1) + N_1 C_v(T_1 - T_0) + m_{AC} C_{AC}(T_1 - T_0)] \end{aligned} \tag{17}$$

where $T_1 = T_{ads}$, $T_2 = T_{ads}$; $n_1$, $n_2$ are amounts of $CO_2$ (moles) in the solid phase (adsorbed) (see Table 2); $N_1$, $N_2$ are amounts of $CO_2$ (moles) in the gas (desorbed) (see Table 2); and $m_{AC}$ = 1 kg and $C_{AC}$ = 900 J/kg·K [18] are the mass and specific heat capacity of activated carbon, respectively.

The heat consumed at isothermal expansion along with desorption (Points 2-3) increases in internal energy $\Delta I_{2\text{-}3}$ and generation of mechanical work $A_{2\text{-}3}$ as follows:

$$T_2 = T_3 = T_{ds} \tag{18}$$

$$Q_{2-3} = \Delta I_{2-3} + A_{2-3} \tag{19}$$

$$\Delta I_{2-3} = [n_3 I_{CO2-AC}(T_3) + N_3 C_v(T_3 - T_0)] - [n_2 I_{CO2-AC}(T_2) + N_2 C_v(T_2 - T_0)] \tag{20}$$

$$A_{2-3} = \int_{V_2}^{V_3} P\, dV \approx \frac{P_2 + P_3}{2}\,(V_3 - V_2) \tag{21}$$

$Q_{3\text{-}4}$, $\Delta I_{3\text{-}4}$, $Q_{4\text{-}1}$, $\Delta I_{4\text{-}1}$, $A_{4\text{-}1}$ are calculated similarly. Note that negative values correspond to the heat release and mechanical work from adsorption and gas compression, respectively. The calculated energy-related parameter are shown in Table 3.

**Table 3** Energy balances along with adsorption-desorption cycle in Figure 6 and Figure 7.

| Trajectory/Parameters | **ΔI, kJ/kg_AC** | **A, kJ/kg_AC** | **Q, kJ/kg_AC** |
|---|---|---|---|
| Desorption | | | |
| Points 1-2 | 249.8 | 0 | 249.8 |
| Points 2-3 | 62.9 | 63.8 | 126.7 |
| Total heat consumed | | | 376.5 |
| Adsorption | | | |
| Points 3-4 | -231.4 | 0 | -231.5 |
| Points 4-1 | -81.2 | -32.3 | -113.5 |
| Total heat released | | | -345.0 |
| **Heat engine balance** | | **31.5** | **31.5** |

The available (useful) work ΔA is obtained as a difference between absolute values of expansion and compression works and can be used to generate power. As shown in Table 3, the energy balance is met because ΔA is equal to the difference between absolute values of consumed and released heats in desorber and adsorber, respectively, as follows:

$$\Delta A = Q_{ds} - Q_{ads} \tag{22}$$

Thermal efficiency $\zeta_{th}$ of the heat engine is defined as work ΔA per consumed heat $Q_{ds}$ and is expressed as follows:

$$\zeta_{th} = \frac{\Delta A}{Q_{ds}} = \frac{31.5}{376.5} = 0.084(8.4\%) \tag{23}$$

Note that the value of consumed heat $Q_{ds}$ is rather conservative without accounting for heat regeneration.

Specific work $\Delta A_m$ per weight of working fluid ($CO_2$ in gaseous phase) is expressed as follows:

$$\Delta A_m = \frac{\Delta A}{M_{CO2}(N_{max} + N_{min})} = \frac{31.5}{44 * (10 + 20.6) * 10^{-3}} = 23.4 \frac{kJ}{kg_{CO_2}} \quad (24)$$

where $M_{CO2}$ is molecular weight of $CO_2$ (44 g/mol); $N_{max}$ + $N_{min}$ is the sum of maximum and minimum molar amounts of $CO_2$ in the gas at $P_{eq}$ in desorber and adsorber, respectively. This specific work indicates an ability of the gas (working fluid) to generate useful work ΔA.

Note that energy balance is carried out without accounting for heat regeneration.

## 4. Results and Discussion

### *4.1 Adsorption-Desorption Cycle in Comparison with Stirling, Carnot, ORC, and Rankine Engines*

The ideal Stirling cycle also consists of two isochores and two isobars, but it fundamentally differs due to an unchanged amount of gas $N_S$ in the cycle. For a clear presentation on P-V diagram in Figure 7, this value is arbitrarily taken as equal to the maximum amount of gaseous $CO_2$ in desorber, as follows:

$$N_s = const = 20.6\, mol \quad (25)$$

Assigning the same temperature range $T_{min} = T_{ads} = 309$ K, $T_{max} = T_{ds} = 309$ K and $P_{eq} = 1500$ kPa, unknown pressures ($P^s_{max}$, $P^s_{min}$) and volumes ($V^s_{max}$, $V^s_{min}$) can be calculated using the Clapeyron-Mendeleev equation. The calculated parameters of the Stirling cycle are presented in Figure 7 (cycle 5-6-3-7).

The well-known analytical expressions for available (useful) work $\Delta A_S$ and consumed heat $Q_S$ in the Stirling cycle without heat regeneration are as follows [19]:

$$\Delta A_s = R(T_{max} - T_{min}) \ln \frac{V^s_{max}}{V^s_{min}} = 0.156 \frac{kJ}{mol} \quad (26)$$

$$Q_s = C_v(T_{max} - T_{min}) + RT_{max} \ln \frac{V^s_{max}}{V^s_{min}} = 3.095 \frac{kJ}{mol} \quad (27)$$

Respectively, thermal efficiency $\zeta^s_{th}$ and specific work are equal, as follows:

$$\zeta^s_{th} = \frac{\Delta A_s}{Q_s} = 5.0\% \quad (28)$$

$$\Delta A^s_m = \frac{\Delta A_s}{10^{-3} M_{CO2}} = 3.55 \frac{kJ}{kg_{CO_2}} \quad (29)$$

Note that both thermal efficiency $\zeta^s_{th}$ and specific work $A^s_m$ are independent of the total amount of gas in the cycle. A significantly higher thermal efficiency $\zeta_{th}$ and specific work $A_m$ of adsorption-desorption cycle obtained under the same conditions indicates a positive impact of the adsorption-desorption mechanism on the efficiency of the useful work generated.

The Carnot efficiency of an ideal, reversible thermodynamic cycle between $T_{min}$ = 309 K and $T_{max}$ = 390 K is 20.8% vs. 8.4% obtained in the absorption-desorption cycle. Recalling that a constant amount of gaseous $CO_2$ in the cycle ($N_{min}$) is always present in adsorber and desorber, it will be of interest to see if reducing its value allows the cycle efficiency to approach the Carnot value.

Table 4 demonstrates increasing efficiency indicators with decreasing $N_{min}$ in the cycle. At the same $P_{eq}$ = 1500 kPa, the difference between $P_{min}$ and $P_{max}$ increases with a decrease in gas volume. At $N_{min} = 4\frac{\text{mol}}{\text{kg\_AC}}$ in adsorber, the thermal efficiency of the adsorption-desorption cycle exceeds more than twice and specific work more than ten times the efficiency and specific work of Stirling engine, respectively.

**Table 4** Parameters and efficiency indicators of adsorption-desorption cycle at decreasing $N_{min}$ and $P_{eq}$ = 1500 kPa per one kg of AC in desorber and adsorber.

| $N_{min}$, mol/kg_AC | $N_{max}$, mol/kg_AC | $V_{min}$, L/kg_AC | $V_{max}$, L/kg_AC | $P_{min}$, kPa | $P_{max}$, kPa | $\zeta_{th}$, % | $\Delta A$, kJ/kg_AC | $\Delta A_m$, kJ/kg_$CO_2$ |
|---|---|---|---|---|---|---|---|---|
| 20 | 30.6 | 34.3 | 66.1 | 938 | 2633 | 6.7 | 27.0 | 12.1 |
| 10 | 20.6 | 17.1 | 44.5 | 857 | 3158 | 8.4 | 31.5 | 23.4 |
| 6 | 16.6 | 10.3 | 35.9 | 809 | 3671 | 9.9 | 36.6 | 36.9 |
| 4 | 14.6 | 6.9 | 31.6 | 779 | 4139 | 11.3 | 41.5 | 50.7 |

Tarrad's [20] thermodynamic analysis of ORCs with different working fluids presented thermal efficiencies ($\zeta_{th}$) in the range of 7.6-8.5%. Certain ORC enhancements increase their thermal efficiencies to about 12.6% [21]. The proposed adsorption-desorption heat engine retains the same efficiency indicators and could compete with ORCs due to an absence of expensive turbines or expanders.

To compare adsorption-desorption and water-steam Rankine cycle efficiencies, the quality of incoming heat should be considered. In other words, available work should be given per unit of exergy. For the case in the last row of Table 4, the exergy of the hot air sensible heat accepted in desorber is as follows:

$$\mathrm{E_{air}} = \mathrm{Q_{air}}\left(1 - {}^{\mathrm{T_0}}/_{\mathrm{T^*}}\right) = 120.2\frac{kJ}{kg_{AC}} \tag{30}$$

where $Q_{air} = Q_{ds}$ = 367.3 *kJ/kg_AC* and an average thermodynamic temperature of air is $T^*$ = 443 *K* (see Chapter 3.1). The exergy efficiency of the cycle is expressed as follows:

$$\zeta_{ex} = \frac{\Delta A}{E_{air}} = \frac{41.5}{120.2} = 0.345(34.5\%) \tag{31}$$

The most sophisticated Rankine cycles transform only 40% of the fuels' (coal, natural gas) heating values into work [22], and their lower heating values are very close to their exergies [23]. The obtained exergy efficiency of adsorption-desorption cycle corresponds well to the exergy efficiency of a regular Rankine cycle unit.

### *4.2 An Available Work to Charge a Spring Mechanism*

The power generation mechanism can be envisioned as a set of similar parallel tubes with two springs and a piston-magnet between them, as shown in Figure 1, Figure 2, and Figure 8 (for clarity, the copper coils are not pictured there). Assume that all springs have the same spring constants (K).

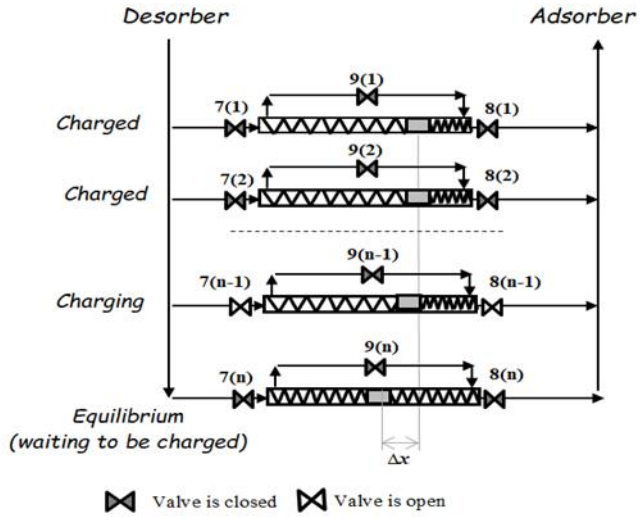


**Figure 8** A set of "n" consecutively charged power generation tubes (see Figure 2 and Figure 3). For clarity, copper coils are not shown.

Thermal oil pushes a piston-magnet and charges springs consecutively - after displacement Δ*x* is reached in one tube, that tube gets closed, and charging continues in the next tube. The potential energy ΔE of springs is a function of displacement Δ*x* and is expressed as follows:

$$\Delta E = nK(\Delta x)^2 \tag{32}$$

where Δ*x* is a positive displacement from equilibrium for both springs and n is the number of tubes.

The available work Δ*A* of the adsorption-desorption cycle is converted into potential energy of springs as follows:

$$\Delta A = \int_{V_2}^{V_3} PdV - \int_{V_4}^{V_1} PdV \approx \frac{P_2 + P_3}{2}(V_3 - V_2) - \frac{P_1 + P_4}{2}(V_4 - V_1) = nK(\Delta x)^2 \tag{33}$$

where, as seen in Figure 7:

$$\Delta \mathrm{V} = (\mathrm{V}_3 - \mathrm{V}_2) = (\mathrm{V}_4 - \mathrm{V}_1) = 27.7\mathrm{L} \tag{34}$$

In the frame of thermodynamic analysis: (i) a relatively small pressure difference between $P_3$ and $P_1$ due to different levels of thermal oil in Vessel_1 and Vessel_2 is neglected; and (ii) an indefinite number of tubes with a very small spring constant K is assumed. This allows application of the following equation:

$$P_3 = P_1 = P_{eq} \tag{35}$$

Substituting (35) and (34) into (33), an expression of springs' potential energy is as follows:

$$\Delta A = \left(\frac{P_2 - P_4}{2}\right)\Delta V = \left(\frac{P_{max} - P_{min}}{2}\right)\Delta V = nK(\Delta x)^2 \tag{36}$$

As follows from this equation, increasing $P_{max}$ and decreasing $P_{min}$ leads to an increase in available work $\Delta A$ and, as seen in Table 4, $\Delta A$ grows despite a decrease in $\Delta V$ with decreasing $N_{min}$.

At finite numbers of tubes $P_3$ - $P_1 \neq 0$ the thermodynamic cycle may look like 1-2-3'-4' (Figure 7), with the following balance of forces in the last tube:

$$(P_3' - P_1)\frac{\pi d^2}{4} = 2K\Delta x \tag{37}$$

ΔV' of the cycle 1-2-3'-4' is expressed as follows:

$$\Delta V' = (V_3' - V_2) = (V_4' - V_1) \tag{38}$$

Furthermore, ΔV' should equal the following:

$$\Delta V' = n\frac{\pi d^2}{4}\Delta x \tag{39}$$

where d is an inner diameter of power generation tubes.

## 5. Conclusion

A new power generation heat engine based on adsorption-desorption cycle to utilize low-temperature waste heat (<250°C) is proposed. The sensible heat of air wasted at temperature 500 K (227°C) and $CO_2$ adsorption on activated carbon were selected as a case to conduct thermodynamic analysis. The heat engine accepts heat at a higher temperature in desorber and releases it at a lower temperature in adsorber. For a continuous semi-batch operation, a switch between desorber and adsorber functionalities is required.

Thermodynamic analysis of the heat engine cycle is carried out for the pair adsorbant-adsorbent: $CO_2$-activated carbon. Its efficiencies are calculated accepting the ideal gas law and an adsorption-desorption equilibrium at the key points of the cycle. The cycle consists of two isochores and two isotherms like that of the Stirling engine, but at the same temperature range and without heat regeneration, its thermal efficiency (work per heat supplied) can reach 11.3% vs. 5.0% and specific work $50.7\frac{kJ}{kg\_CO2}$ vs. $3.55\frac{kJ}{kg\_CO2}$ in the latter. These dramatic increases in efficiencies result from the fact that the expansion work is increased due to $CO_2$ desorption and the compression work is decreased due to $CO_2$ adsorption to the adsorbent.

The proposed unit has thermal efficiency in the range of Organic Rankine Cycle units and can be utilized in small-scale applications up to 40 kWe, where manufacturing cost of turbines or expanders for ORCs increases dramatically. Accounting for quality (temperature) of utilized heat,

the exergy efficiency of the proposed cycle $\zeta_{ex}$ = 34.5% approaches that of water-steam Rankine cycles utilizing natural gas or coal combustion.

An experimental kinetic study is needed to obtain the heat engine capacity (wattage) in response to the frequency of switching between desorber and adsorber. The selection of an advanced adsorbant-adsorbent pair should be based on the temperature of waste heat and the required capacity.

**Nomenclature**

| | |
|---|---|
| A | work generated and consumed in the cycle, kJ/kg_AC |
| ΔA | work produced as a difference between generated and consumed works in the cycle, kJ/kg_AC |
| $\Delta A_m$ | specific work (per kg of working fluid) produced in the cycle, kJ/kg_$CO_2$ |
| $\Delta A_s$ | work produced by Stirling engine, kJ/mol_$CO_2$ |
| $\Delta A_m^s$ | specific work (per kg of working fluid) produced by Stirling engine, kJ/kg_$CO_2$ |
| *b, $b_0$* | adsorption affinity and adsorption affinity at infinite temperature, $kPa^{-1}$ |
| $C_{AC}$ | activated carbon heat capacity, J/(kg·K) |
| $C_p^{air}$ | isobaric heat capacity of air, J/(mol ·K) |
| $C_p$ | isobaric heat capacity of $CO_2$, J/(mol· K) |
| $C_v$ | isochoric heat capacity of $CO_2$, J/(mol· K) |
| dH | differential change in air enthalpy, J/mol |
| dS | differential change in air entropy, J/(mol·K) |
| d | diameter of power generation tubes, m |
| $E_{air}$ | exergy of air, J/mol; kJ/kg_AC |
| $E_{sv}$ | exergy of saturated vapor produced by cooling of one mole of air, J/mol_air |
| H | enthalpy, J/mol |
| I | internal energy of $CO_2$ along the cycle, J/mol |
| $I_{CO2\text{-}AC}$ | internal energy of adsorbed $CO_2$, J/mol |
| ΔI | change of internal energy in desorber and adsorber, kJ/kg_AC |
| $M_{CO2}$ | molar mass of $CO_2$, 44 g/mol |
| $m_{AC}$ | activated carbon mass in adsorber and desorber, 1 kg |
| K | spring constant, N/m |
| $N_S$ | amount of $CO_2$ in Stirling cycle, mol |
| N | amount of $CO_2$ in gas per kg of activated carbon, mol/kg_AC |
| n | amount of adsorbed $CO_2$ per kg of activated carbon, mol/kg_AC |
| n | number of power generation tubes in a set |
| Q | heat released or consumed, J/mol or kJ/kg_AC |
| q, $q_0$ | mass and saturated mass of adsorbed $CO_2$ by unit mass of adsorbent, kg/kg |
| P | pressure, kPa and Bar |
| *R* | universal gas constant, 8.314 J/(mol·K) |
| *T* | temperature, K or °C |
| $T_0$ | reference temperature, 298K |
| $T^*$ | average thermodynamic temperature, K |
| *t* | heterogeneity parameter |

| | |
|---|---|
| $V$ | volume, L |

**Greek Symbols**

| | |
|---|---|
| Δx | springs displacement |
| Δ | difference |
| $\zeta_{th}$ | thermal efficiency of adsorption-desorption cycle |
| $\zeta_{ex}$ | exergetic efficiency of adsorption-desorption cycle |
| $\zeta_{th}^{S}$ | thermal efficiency of Stirling cycle |

**Subscripts**

| | |
|---|---|
| AC | activated carbon |
| ads | adsorption |
| air | air |
| $CO_2$-AC | adsorbed $CO_2$ on activated carbon |
| ds | desorption |
| eq | equilibrium |
| in | input |
| min | minimum |
| max | maximum |
| out | output |
| sv | saturated vapor |
| 1, 2, 3, 4, 3', 4', 5, 6, 7 | cycle points |

**Superscripts**

| | |
|---|---|
| AC | activated carbon |
| s | Stirling engine |

**Abbreviations**

| | |
|---|---|
| AC | activated carbon |
| ORC | Organic Rankine Cycle |

**Author Contributions**

The author conducted all the research work for this study.

**Competing Interests**

There are no conflicts to declare.

**References**

1. Quoilin S, van den Broek M, Declaye S, Dewallef P, Lemort V. Techno-economic survey of Organic Rankine Cycle (ORC) systems. Renew Sustain Energy Rev. 2013; 22: 168-186.

2. Klonowicz P, Witanowski Ł, Jędrzejewski Ł, Suchocki T, Lampart P. A turbine based domestic micro ORC system. Energy Procedia. 2017; 129: 923-930.
3. Tocci L, Pal T, Pesmazoglou I, Franchetti B. Small scale Organic Rankine Cycle (ORC): A technoeconomic review. Energies. 2017; 10: 413. doi: 10.3390/en10040413.
4. Colonna P, Casati E, Trapp C, Mathijssen T, Larjola J, Turunen Saaresti T, et al. Organic rankine cycle power systems: From the concept to current technology, applications, and an outlook to the future. J Eng Gas Turbines Power. 2015; 137: 100801. doi: 10.1115/1.4029884.
5. Durcansky P, Nosek R, Jandacka J. Use of stirling engine for waste heat recovery. Energies. 2020; 13: 4133. doi: 10.3390/en13164133.
6. Zhu S, Yu G, Liang K, Dai W, Luo E. A review of stirling-engine-based combined heat and power technology. Appl Energy. 2021; 294: 116965.
7. Shabir F, Sultan M, Miyazaki T, Saha BB, Askalany A, Ali I, et al. Recent updates on the adsorption capacities of adsorbent-adsorbate pairs for heat transformation applications. Renew Sust Energy Rev. 2020; 119: 109630.
8. Chauhan PR, Kaushik SC, Tyagi SK. Current status and technological advancements in adsorption refrigeration systems: A review. Renew Sust Energy Rev. 2022; 154: 111808.
9. Nomura K, Ishido Y, Ono S. A novel thermal engine using metal hydride. Energy Convers. 1979; 19: 49-57.
10. Bao H, Wang Y, Roskilly AP. Modelling of a chemisorption refrigeration and power cogeneration system. Appl Energy. 2014; 119: 351-362.
11. Muller AW, Schulze Makuch D. Sorption heat engines: Simple inanimate negative entropy generators. Physica A. 2006; 362: 369-381.
12. Darvish K, Ehyaei MA, Atabi F, Rosen MA. Selection of optimum working fluid for organic rankine cycles by exergy and exergy-economic analyses. Sustainability. 2015; 7: 15362-15383. doi: 10.3390/su71115362.
13. Duratherm. Duratherm LT [Internet]. Tonawanda, NY, US: Duratherm; 2022. Available from: https://durathermfluids.com/products/duratherm-lt.
14. Velisa V. Pentane [Internet]. Thermopedia; 2011. doi: 10.1615/AtoZ.p.pentane. Available from: https://www.thermopedia.com/content/1016/.
15. Dincer I, Rosen MA. Exergy: Energy, Environment and Sustainable Development. 3rd ed. Amsterdam, Netherlands: Elsevier Science; 2020.
16. Jribi S, Miyazaki T, Saha BB, Pal A, Younes MM, Koyama S, et al. Equilibrium and kinetics of $CO_2$ adsorption onto activated carbon. Int J Heat Mass Transf. 2017; 108: 1941-1946.
17. Saha P, Chowdhury S. Insight into adsorption thermodynamics [Internet]. London, UK: IntechOpen; 2011. Available from: http://www.intechopen.com/books/thermodynamics/insight-into-adsorption-thermodynamics.
18. Uddin K, Islam MA, Mitra S, Lee JB, Thu K, Saha BB, et al. Specific heat capacities of carbon-based adsorbents for adsorption heat pump application. Appl Therm Eng. 2018; 129: 117-126.
19. Singh O. Applied Thermodynamics. 3rd ed. New Delhi, India; New Age International Publisher; 2009.
20. Tarrad AH. A steady-state evaluation of simple organic rankine cycle (SORC) with low-temperature grade waste heat source. J Power Energy Eng. 2020; 8: 15-31.

21. Wang R, Jiang L, Ma Z, Gonzalez Diaz A, Wang Y, Roskilly AP. Comparative analysis of small-scale organic rankine cycle systems for solar energy utilisation. Energies. 2019; 12: 829.
22. Muller Steinhagen, Gottfried HM. Rankine Cycle [Internet]. Thermopedia; 2011. doi: 10.1615/AtoZ.r.rankine_cycle. Available from: https://www.thermopedia.com/content/1072/.
23. Haseli Y. Entropy Analysis in Thermal Engineering System. Cambridge, MA, US: Academic Press; 2019.